POLITECNICO
MILANO 1863

SCUOLA DI INGEGNERIA INDUSTRIALE
E DELL'INFORMAZIONE

EXECUTIVE SUMMARY OF THE THESIS

Innovative techniques for neural stimulation using magneto-electric nanoparticles

TESI MAGISTRALE IN BIOMEDICAL ENGINEERING – INGEGNERIA BIOMEDICA

AUTHOR: Anna Tommasini

ADVISOR: Paolo Giuseppe Ravazzani

CO-ADVISOR: Giulia Suarato, Alessandra Marella

ACADEMIC YEAR: 2023-2024

1. Introduction

In the field of medical interventions, electrical stimulation is emerging as a key therapeutic modality, demonstrating considerable advantage in nerve stimulation for restoring motor function and relieving chronic pain. The interdisciplinary field of neurotechnology explores new ways of interfacing with the human nervous system, fostering personalized functional solutions through innovations such as neuroprostheses, which include several components, such as electrical stimulators, electrodes, control sensors, and optional orthoses[1]. There are different types of stimulation electrodes, from implanted to transcutaneous variants, which differs in invasiveness, selectivity, and cost. In this context, electrical stimulation triggers action potentials in nerves by depolarizing ion channels, thus initiating neuronal depolarization and subsequent generation of action potentials. In this context, nanomedicine explores nanotechnological strategies for therapeutic and diagnostic purposes. Magnetoelectric nanoparticles (MENPs) represent a recent target in this field, offering wireless and high-level stimulation capabilities [2]. When MENPs are subjected to a low-intensity magnetic field, their ferromagnetic core undergoes a magnetic alignment process that causes its deformation, which then propagates to the piezoelectric shell, mechanically connected to the core, thus generating an electric field [3]. This magnetoelectric coupling between the magnetostrictive core and the piezoelectric shell is defined through the coefficient αME = $\Delta E/\Delta H$ [V/cmOe] [4]. MENPs already showed remarkable potential *in vivo*, generating highly localized electric fields approaching the neural activation threshold (100 V/m) [5]. However, the rapid spatial decay of the electric field generated remains a challenge that requires further exploration and optimization [6]. In the early stages of designing new medical devices for neurostimulation, computational modeling emerges as a valuable tool to investigate device properties and address bioelectromagnetic challenges. Adhering to the principle of 3Rs (reduce, refine, replace), computational approaches reduce the need to conduct extensive animal experiments, improve

the quality of research, and optimize resource utilization. Leveraging previous research on MENPs design, our project aims to establish a multi-scale in silico model to generate an effective stimulation by incorporating MENPs into a biocompatible 3D polymer matrix to overcome the limitations of the spatial decay of MENPs electric signal. An advanced computational model enabled the optimization and functional evaluation of the magnetoelectric patch here described, thus representing a significant step toward the development and fabrication of innovative MENPs-based biocompatible patches for the treatment of neurological disorders and the restoration of impaired neuronal function.

2. Materials and Methods

This study evaluates the functionality of MENPs-based composite patches for peripheral nerve stimulation through three key steps, described in the flowchart of Fig. 1. In the model, MENPs at the concentration of 18 wt% are embedded in a 3D polymeric matrix.

Fig. 1 Simulations Step Flowchart.

Firstly, simulations at the nanoscale are conducted to evaluate the capability of three different polymers to propagate the electric fields generated by the MENPs. Next, micrometer-scale structures are analyzed to evaluate the electrical features of the composite patch by increasing the scale. Finally, more clinically-size millimeter-scale models are examined to study the generation of electric fields in real nerve environments, subsequently translating them into neuronal responses using a specialized software interface. All simulations were performed with the Sim4life platform (by ZMT Zurich Med Tech AG, Zurich, Switzerland, www.zurichmedtech.com).

2.1. Nanometric Model

Sim4Life was the used platform, and it resolves the low-frequency electromagnetic problem using the ohmic quasi-static approximation, a numerical technique within the finite element method (FEM). This approach is particularly useful for solving partial differential equations in complex geometries where analytical methods are impractical. Through FEM, the Laplace equation used to obtain the electric potential (ϕ) becomes: $\nabla\cdot(\sigma\nabla\phi) = 0$. Where σ (S/m) is the electrical conductivity of tissues set according to the stimulating frequency. Following previous research works, the chosen frequency is 100 Hz, which is commonly adopted for neural stimulation studies, as reported in the literature [7]. Then, the E field distribution was derived by means of the following relation: $E = -\nabla\phi$. The model encompassed three subdomains: 3D magnetoelectric nanoparticles (MENPs), a cubic polymer matrix, and surrounding tissue (Fig. 2). To represent the magnetoelectric effect of MENPs, a spherical structure with a 90 nm diameter was chosen, with its distribution exhibiting a dipolar configuration. This was modeled by two hemispheres, one with a positive electric potential of *+2.25 mV* and the other with a negative potential of *-2.25 mV*. The insulating layer between the two caps was composed of Tecothane 75D, with dielectric properties tailored according to the stimulation frequency, as reported on the left side of Fig. 2.

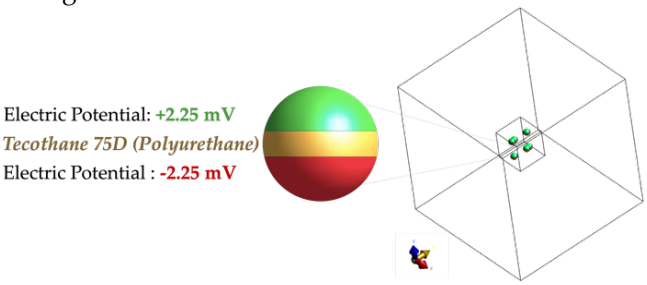

Fig. 2 on the left: MENP model in Sim4life red shell with V= - 2.25 mV, green shell with V= + 2.25 mV, and middle layer Tecothane 75D material in yellow; on the right: The three subdomains of the model: six magnetoelectric nanoparticles (MENPs), a cubic polymer matrix, and surrounding tissue.

Within the cubic polymer matrix measuring 400 nm on each side, six MENPs were arranged to ensure uniform distribution and maximize the magnetoelectric effect. This composite was then embedded within a larger cubic domain representing nerve tissue, with electrical properties predefined according to the materials database of the software. Three simulations were conducted, each varying the polymer matrix (polycaprolactone (PCL), poly(3-hexylthiophene) (P3HT) and a mixture of silk fibroin and polypyrrole (SF-PPy). Qualitative evaluation of potential and current density at the polymer

surface was carried out, followed by a quantitative analysis of statistical parameters using MatlabR2023b and OriginPro2022.

2.2. Micrometric Model

Once the optimal material was identified from those previously analyzed, the study moved to a micrometer-scale structure. This is a significant step to evaluate how the electrical properties of repeated nanometer units affects the overall electrical performance of a larger micrometer assembly. Two models were designed, which incorporated three and four basic units in each spatial dimension, for a total of 27 and 64 basic units, respectively. The resulting microstructures had cubic shapes with sides of 1.2 μm and 1.6 μm, housing inside 165 and 384 MENPs. As with the nanometer model, the two structures are embedded in a larger volume of 2 μm side with characteristics similar to those of the nerve tissue. At the stimulation frequency of 100 Hz, a comparison was made between the nanometer base unit and the two microstructures. In particular, the distributions of current density and electric potential developed on the surface of the models were studied to evaluate their behaviors.

2.3. Millimetric Model

2.3.1. Electromagnetic Stimulation

To overcome the computational constraints of the software, which cannot handle calculations with many basic units, the simplification of using the layout implemented at the nanometric scale also for the millimetric model was adopted. This approach involved considering a volume fraction of 0.04 and calculating a scaling factor to determine the radius and reciprocal positioning of the magnetoelectric nanoparticles, thus ensuring the proportionality between the two models. The millimeter model was designed by keeping the surface current density values constant. A cylindrical nerve model already present in the Sim4Life platform was imported, to ensure an accurate representation of the true tissue proportions, relative to the millimeter electrode. The model includes subdomains representing different tissues, each with distinct electrical characteristics, automatically updated by the software database according to the stimulation frequency. The ME-patch is placed in contact with the nerve model and encapsulated in a silicone layer to isolate the electrode from the surroundings and to ensure that the electric charges are channeled towards the nerve fibers. The electric field in the nerve cross section is examined in relation to six different orientations assumed each time by the ME-patch.

2.3.2. Neuron Dynamic

The Sim4Life computational simulation platform includes the NEURON solver, which implements models of electrical signaling of individual neurons. The platform simulates the wire equations that describe nerve cells and solves them computationally. The MOTOR model, which represents the dynamics of peripheral nerves, was used in this study. It includes explicit representations of Ranvier's nodes, paranodal and internodal sections of the axon, and a myelin sheath with finite impedance [8]. The pulse used for nerve stimulation is a sine wave with an amplitude obtained from electromagnetic simulation and a frequency of 100 Hz. Several simulations were conducted by orienting the patch in various ways to study its stimulating effect according to its rotation and nerve reciprocal positioning.

3. Results & Discussion

Perfectly in line with the increasing interest in novel methods of peripheral nervous system (PNS) stimulation, this study explores the potentiality of using a 3D polymer matrix embedded with magnetoelectric nanoparticles (MENPs). Through an *in silico* approach, the electrical performance of the ME-Patch is optimized, starting with a nanoscale modeling in which the material to be used is thoroughly investigated, to obtain a functional evaluation of the proposed structure with a realistic peripheral nerve model.

3.1. Nanometric Structure

The electrical characteristics of three different polymer formulations were examined in relation to the magnetoelectric effect of MENPs. The study adopts biocompatible materials suitable for various biotechnological applications, either of synthetic origin, such as polycaprolactone (PCL), poly(3-hexylthiophene) (P3HT), or naturally-derived materials, such as the silk fibroin-polypyrrole (SF-PPy) blend, thus covering a wide range of electrical conductivity values ($\sigma_{PCL} = 1 \times 10^{-6}$ S/m, $\sigma_{SF\text{-}PPy} = 80$ S/m, $\sigma_{P3HT} = 2.24 \times 10^{4}$ S/m). The simulations conducted showed significant

differences in the electrical potential distribution among the nanocomposites. The three systems were qualitatively analyzed, and the MENPs-P3HT one showed the highest electrical potential conductivity (as shown in Fig. 3); in particular, proper activation of the nanoparticles within the matrix can be appreciated, followed by efficient electrical potential propagation. The MENPs-SF-PPy composite behaves similarly to the previous one, while MENPs-PCL showed poor propagation of electric potential produced by the nanoparticles, whose values are close to zero on the surface.

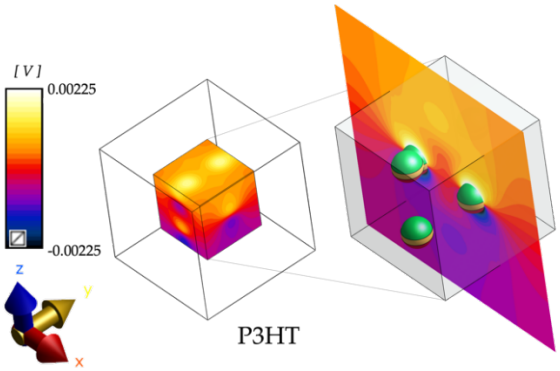

Fig. 3 Electric Potential profiles on the matrix made of poly (3-hexylthiophene (P3HT) which contains MENPs. On the right, the profile in cross-section on the xz plane (representing the base unit center) is shown.

Statistical values for the current density distributions among different polymers are given in the Table 1 below.

Table 1 Statistical analysis on different adopted polymers (polycaprolactone (PCL), poly(3-hexylthiophene) (P3HT) and a mixture of silk fibroin and polypyrrole (SF-PPy)

J [A / m²]	PCL	SF-PPy	P3HT
Mean	3.04×10^{-2}	7.66×10^{3}	7.70×10^{3}
Median	2.16×10^{-2}	4.52×10^{3}	4.54×10^{3}
Max	1.41×10^{-1}	3.91×10^{4}	3.98×10^{4}
Min	2.22×10^{-4}	7.69×10^{1}	7.89×10^{1}

This confirmed the robust electrical performance of the MENPs-P3HT system, with values with orders of magnitude significantly higher than the other two materials, suggesting this composite as the most promising candidate for further investigations.

3.2. Micrometric Structure

To understand how the collective behavior affects the overall electrical performance, the potential distribution and current density of a micrometric structrure were examined. Despite the structure being gradually larger, from Fig. 4,the maintenance of a dipolar behavior can be appreciated by noticing the presence of one face of the volume at a more positive potential (mostly colored in *yellow*) and one at a more negative potential (predominantly colored in *purple*).

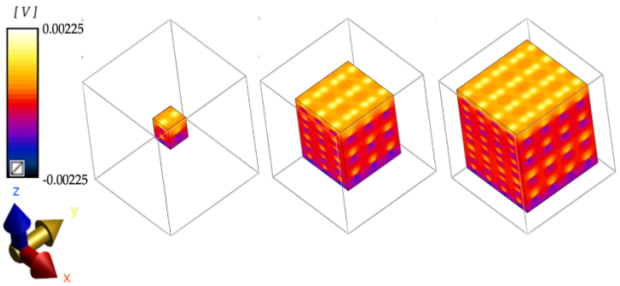

Fig. 4 Electrical Potential distribution at the outer surface of the ME-patch: left - nanometric model (1 base unit, 6 MENPs); center - 1.2 μm side structure (27 base units, 162 MENPs); right - 1.6 μm side structure (64 base units, 384 MENPs).

The current density distributions between the nanometer unit and the two micrometer structures were compared, both qualitatively and quantitatively. The statistical values of this parameter for each structure are shown in the Table 2. Once again, the retention of the values measured in the nanometer model is appreciable, regardless of the size and number of nanoparticles within the structure.

Table 2 Statistical analysis on the current density profiles for the different modelled structures

J [A / m²]	400 nm	1.20 μm	1.60 μm
Mean	1.22×10^{8}	1.16×10^{8}	1.19×10^{8}
Median	8.29×10^{7}	7.77×10^{7}	7.94×10^{7}
Max	8.13×10^{8}	8.90×10^{8}	9.67×10^{8}
Min	4.54×10^{5}	1.11×10^{6}	4.77×10^{5}

The micrometer-sized configurations not only maintained the initial dipolar behavior, but also exhibited the same current density values observed for all the models (nanometer, micrometer with 165 MENP, and micrometer with 384 MENP), demonstrating the preservation of the essential electrical characteristics, despite the increase in scale.

3.3. Millimetric Structure

3.3.1. Electromagnetic Stimulation

The previous findings provide crucial insights for the final stage of the millimeter patch modeling. In this section, the same configuration of the

nanometric model is used, on which an appropriate electrical potential is imposed. This potential will be able to generate a current density similar to that observed in the nanometer structure, previously shown to be constant regardless the increasing number of nanometer units within the structure ($J = 8.29 \times 10^7\ A/m^2$). Three ME-patch sides, symmetric in terms of current density, are analyzed. For each side, two simulations are performed, varying its orientation with respect to the longitudinal axis of the nerve, for a total of 6 configurations of stimulation. The electric field distributions in the nerve tissue and their spatial decay are analyzed, revealing changes in the electric field profile depending on the side of the millimeter patch in contact with the nerve and its orientation. In Fig. 5 the best case (highlighted in pink), where the electric field values reach higher levels and get deeper into the nerve cross-section, and the worst case (highlighted in blue), whose electric field undergoes the fastest spatial decay, are reported.

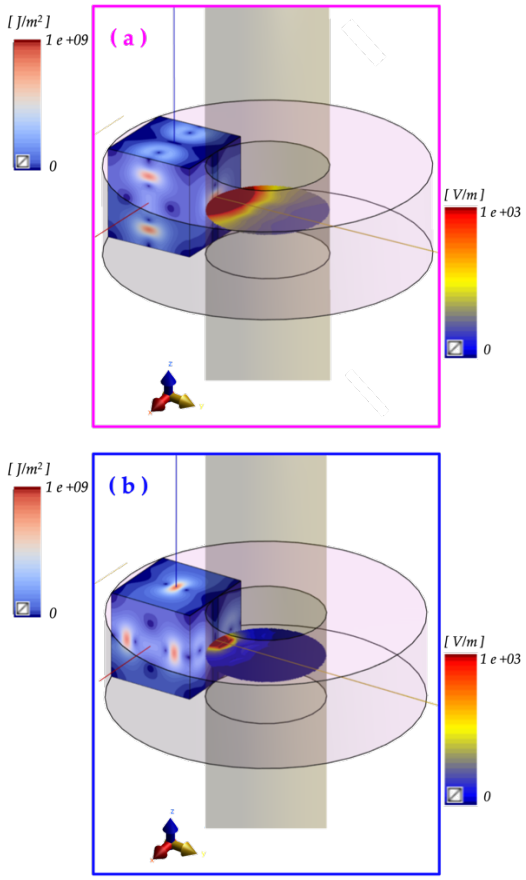

Fig. 5 Two different E_{field} profiles developed within the nerve cross-section, when in contact with (a) the best stimulating side and with (b) the worst stimulation side of the ME-graft.

To support the qualitative considerations, the electric field profiles in the nerve cross-section were further investigated. As in the previous analyses, all six case histories are graphed. Below, only the electric field decay profiles of the best and worst cases are shown (Fig. 6).

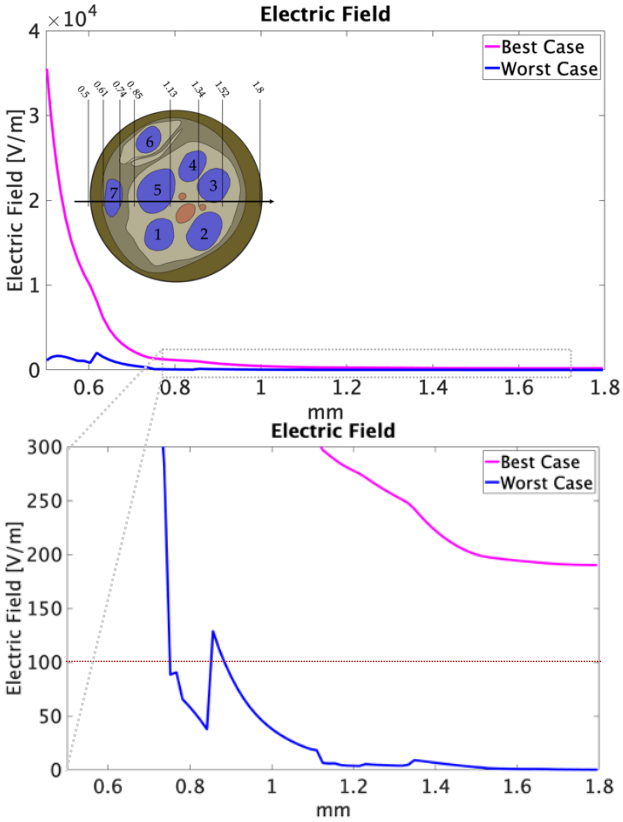

Fig. 6 Spatial decays of electric field (Efield) generated in the cross section of the nerve in the best (in pink) and worst (in blue) cases. Below, a zoom [0-300 V/m] on the electric field decay profile that remains above the threshold (in red) for the best case and below for the worst.

In our best case (Fig.6, pink line), the electric field generated exceeds the threshold values necessary to elicit a neuronal response (100 V/m), suggesting the effectiveness of the millimeter patch in stimulating a model nerve tissue and modulating the neuronal activity. On the contrary, in the "worst case" configuration (Fig.6, blue line) the electric field rapidly decays in the vicinity of the patch, not ensuring an effective stimulation in depth.

3.3.2. Neuronal Dynamics

Neuronal dynamics is studied via Neuron, which uses as input the electric field values obtained from previous electromagnetic simulations. The neuronal response is characterized by the succession of action potentials (APs), consisting of

several phases. A resting state is observed, in which the neural membrane potential is maintained around -80 mV, mainly stabilized by potassium permeability. Following stimulation, the depolarization phase begins with the opening of sodium channels, leading to an increase in the membrane potential up to its peak (near 30-40 mV), known as overshoot. Next, the repolarization phase occurs with the opening of potassium channels and the closing of sodium channels, which lead to the returning the membrane potential to its resting values. The APs shown in Fig. 7 refers to the neuronal response of fascicle 7, defined as the one closest to the electrode, and are related to the two cases reported in the above study (Fig. 5 and Fig. 6).

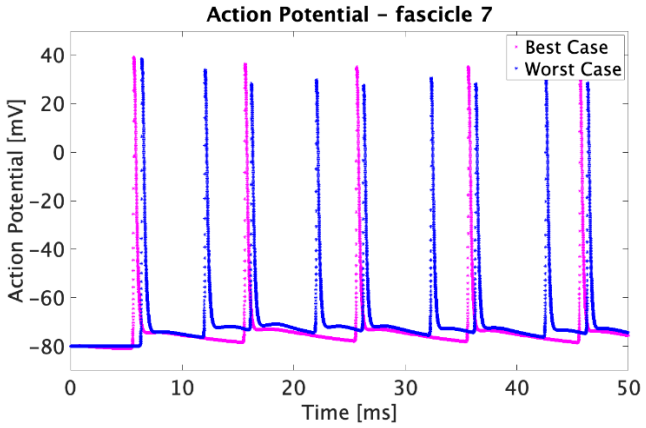

Fig. 7 The APs generated by the best case (pink line) and worst case (blue line) of the above study, related to the neuronal response of fascicle 7, defined as the one closest to the electrode.

The phases of the neuronal response relative to the fascicle closest to the electrode can be observed, confirming that stimulation occurred for the case with slower E_{field} decay (Fig. 7, pink line) and the case with faster E_{field} decay (Fig. 7, blue line). These outcomes suggest that the generation of the action potential is independent from the differences in amplitude of the generated electric fields, if a certain threshold is exceeded. Activation begins at 5 ms, but a different periodicity is observed, prompting possible effects due to the different refractory periods of the two stimulations. In the favorable situation, associated with a more intense and penetrating electric field, a reduced periodicity and a prolonged refractory period are detected. This can be ascribed to the wider negative sinusoidal half-wave input, extending the refractory period compared to the case characterized by a less intense and more rapidly decreasing electric field.

Lastly, the concept of deep stimulation was further investigated. To do so the action potentials related to fascicles 3, 5 , and 7 (nerve cross section in Fig. 6), were plotted for both stimulations (Fig. 8). These fascicles are gradually distant with respect to the electrode and, as a consequence, were affected differently by the electric field generated by the ME-patch.

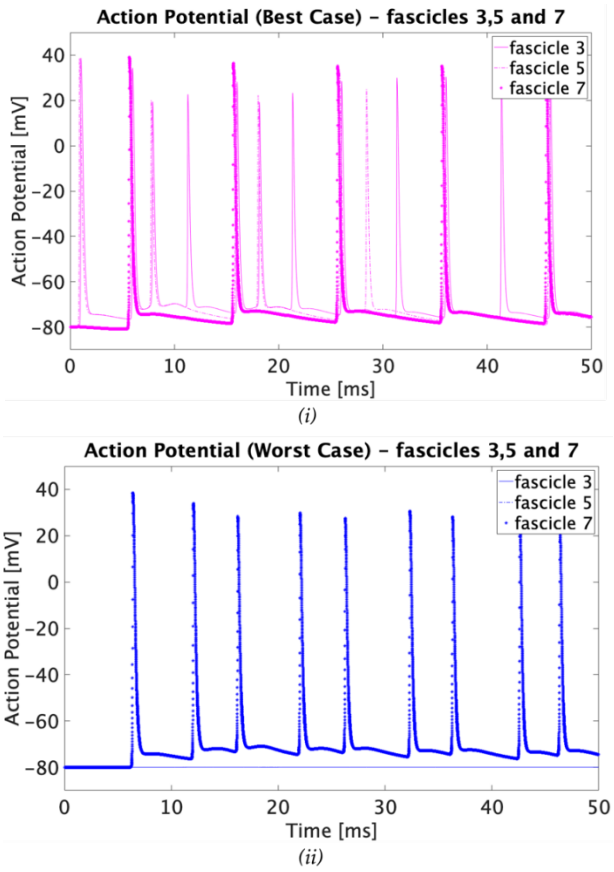

Fig. 8 (i) Action potential (AP) of the fascicle 3, 5, and 7 related to the simulation with the most efficient ME-patch orientation; (ii) Action potential (AP) of the fascicle 3, 5, and 7 related to the simulation with the least efficient ME-patch orientation.

As expected, the best case scenario (Fig. 8i) lead to APs sparking in all fascicles, indicating a deep stimulation. A different periodicity of the APs generated in the various fascicles under study is present, since the stimulation sine wave perceived by the farthest ones is shallower compared to the sine wave sensed by fascicle 7; again, this could be referred to a different refractory period. On the contrary, the worst case configuration (Fig. 8ii), presenting a very rapid E_{field} decay, could elicit a neuronal response only within the fascicle closest to the electrode (fascicle 7), while the other two (fascicle 5 and fascicle 3) were reached by subthreshold values, which were not able to generate action potentials.

4. Conclusion

This study established a comprehensive computational framework for the design of a new wireless electrical stimulation technology with the goal of effectively activating neuronal responses. A three-dimensional, nanostructured magnetoelectric patch was developed by carefully defining the composition of the polymer matrix and the loading concentrations of the magnetoelectric nanoparticles. This optimization is critical to efficiently transmit electricity through a biocompatible wireless system, with the goal of triggering neuronal action potentials and distributing the electric field within a human nerve tissue model. Our methodological approach has enabled accurate simulation of the effectiveness of the magnetoelectric patch in generating neuronal action potentials and modulating the electric field distribution. Future directions include exploring different shapes/geometries of the ME-Patch and implementing modeled voltage structures to better replicate realistic materials, thus improving a deep nerve tissue stimulation. Overall, our results provide a solid scientific basis for the development of novel bioelectric therapies for the treatment of compromised nerve tissue, thus advancing the engineering of magnetoelectric devices for neural interfacing.

References

[1] C. Marquez-Chin and M. R. Popovic, "Functional electrical stimulation therapy for restoration of motor function after spinal cord injury and stroke: A review," *BioMedical Engineering Online*, vol. 19, no. 1. BioMed Central Ltd., May 24, 2020. doi: 10.1186/s12938-020-00773-4.

[2] S. Fiocchi *et al.*, "Modeling of core-shell magneto-electric nanoparticles for biomedical applications: Effect of composition, dimension, and magnetic field features on magnetoelectric response," *PLoS One*, vol. 17, no. 9 September, Sep. 2022, doi: 10.1371/journal.pone.0274676.

[3] A. Marrella *et al.*, "Magnetoelectric nanoparticles shape modulates their electrical output," *Front Bioeng Biotechnol*, vol. 11, 2023, doi: 10.3389/fbioe.2023.1219777.

[4] H. Song, M. A. Listyawan, and J. Ryu, "Core–Shell Magnetoelectric Nanoparticles: Materials, Synthesis, Magnetoelectricity, and Applications," *Actuators*, vol. 11, no. 12. MDPI, Dec. 01, 2022. doi: 10.3390/act11120380.

[5] N. Danner, M. Könönen, L. Säisänen, R. Laitinen, E. Mervaala, and P. Julkunen, "Effect of individual anatomy on resting motor threshold – Computed electric field as a measure of cortical excitability," *J Neurosci Methods*, vol. 203, no. 2, pp. 298–304, Jan. 2012, doi: 10.1016/J.JNEUMETH.2011.10.004.

[6] S. Fiocchi, E. Chiaramello, A. Marrella, M. Bonato, M. Parazzini, and P. Ravazzani, "Modelling of magnetoelectric nanoparticles for non-invasive brain stimulation: a computational study," *J Neural Eng*, vol. 19, no. 5, Oct. 2022, doi: 10.1088/1741-2552/ac9085.

[7] I. Takako Smith *et al.*, "Nanomedicine and nanobiotechnology applications of magnetoelectric nanoparticles," *WIREs Nanomed Nanobiotechnol*, 2023, doi: 10.1002/wnan.1849.

[8] C. C. McIntyre, A. G. Richardson, and W. M. Grill, "Modeling the excitability of mammalian nerve fibers: Influence of afterpotentials on the recovery cycle," *J Neurophysiol*, vol. 87, no. 2, pp. 995–1006, 2002, doi: 10.1152/jn.00353.2001.